

Sources of and Solutions to Problems in the Refinement of Protein NMR Structures against Torsion Angle Potentials of Mean Force

John Kuszewski and G. Marius Clore¹

Laboratory of Chemical Physics, Building 5, National Institute of Diabetes and Digestive and Kidney Diseases,
National Institutes of Health, Bethesda, Maryland 20892-0510

Received April 4, 2000; revised June 7, 2000

It is often the case that a substantial number of torsion angles (both backbone and sidechain) in structures of proteins and nucleic acids determined by NMR are found in physically unlikely and energetically unfavorable conformations. We have previously proposed a database-derived potential of mean force comprising one-, two-, three-, and four-dimensional potential surfaces which describe the likelihood of various torsion angle combinations to bias conformational sampling during simulated annealing refinement toward those regions that are populated in very high resolution (≤ 1.75 Å) crystal structures. We now note a shortcoming of our original implementation of this approach: namely, the forces it places on atoms are very rough. When the density of experimental restraints is low, this roughness can both hinder convergence to commonly populated regions of torsion angle space and reduce overall conformational sampling. In this paper we describe a modification that completely eliminates these problems by replacing the original potential surfaces by a sum of multidimensional Gaussian functions. Structures refined with the new Gaussian implementation now simultaneously enjoy excellent global sampling and excellent local choices of torsion angles.

INTRODUCTION

Protein structure determination by NMR involves the optimization of an underrestrained function. The number and geometric specificity of the available experimental restraints, namely NOE-derived interproton distances, scalar couplings, chemical shifts, and dipolar couplings, are insufficient to determine the structure of a protein in their own right (1). Consequently, the use of *a priori* information in the form of covalent geometry restraints (bond lengths and angles, chirality, and planarity) and a van der Waals term (typically in the form of some sort of simplified repulsive potential to prevent atomic overlap) is an essential prerequisite (1). In two recent papers, we have shown that it is also possible, given the current availability of large numbers of very high-resolution (≤ 1.75 Å) crystal structures, to include larger scale information relating to protein and nucleic acids as *a priori* restraints (2, 3). These restraints are in the form of a database-derived potential

of mean force (4) comprising one-, two-, three-, and four-dimensional potential surfaces which describe the likelihood for various torsion angle combinations (2, 3). Unlike covalent geometry restraints that relate to small-scale structural features and are confined to a single expectation value, the torsion angle potentials of mean force permit several alternative conformational possibilities. This is achieved by biasing the sampling during simulated annealing refinement to conformations that are likely to be energetically possible by effectively limiting the choices of dihedral angles to those that are known to be physically realizable (2). An example of such a restraint is a potential energy term that expresses the likelihood of a particular residue type having a given set of φ/ψ backbone torsion angles and whose surface has minima located in the α -helical, β -sheet, and left-handed helical regions of the Ramachandran plot. Because the potential energy surfaces are created from protein crystal structures, these larger scale conformational database restraints are individually much less precise than traditional covalent geometry restraints, which originate from small molecule X-ray structures at atomic resolution. Even so, we have shown that inclusion of the torsion angle potential of mean force improves the local accuracy of NMR structures significantly without affecting the agreement with the experimental NMR restraints (2, 3).

THE PROBLEM

Experience with our original implementation of the torsion angle potential of mean force (2, 3) (which we will now refer to as “DELPHIC torsions,” for *database-elucidated likelihood ‘phor’ internal coordinates*) has suggested that in certain cases it may be rather difficult to optimize by simulated annealing. For example, in some structures refined against the DELPHIC torsion potential, a small number of residues occasionally appears to be stuck in poor φ/ψ conformations, even though there are no restraints holding them there.

The DELPHIC potential surfaces do not appear to the eye to be rough enough to present difficulties to optimization (Fig. 1a), and indeed one-dimensional slices through these potentials show them to be reasonably smooth (Fig. 1b). The slight

¹ To whom correspondence should be addressed.

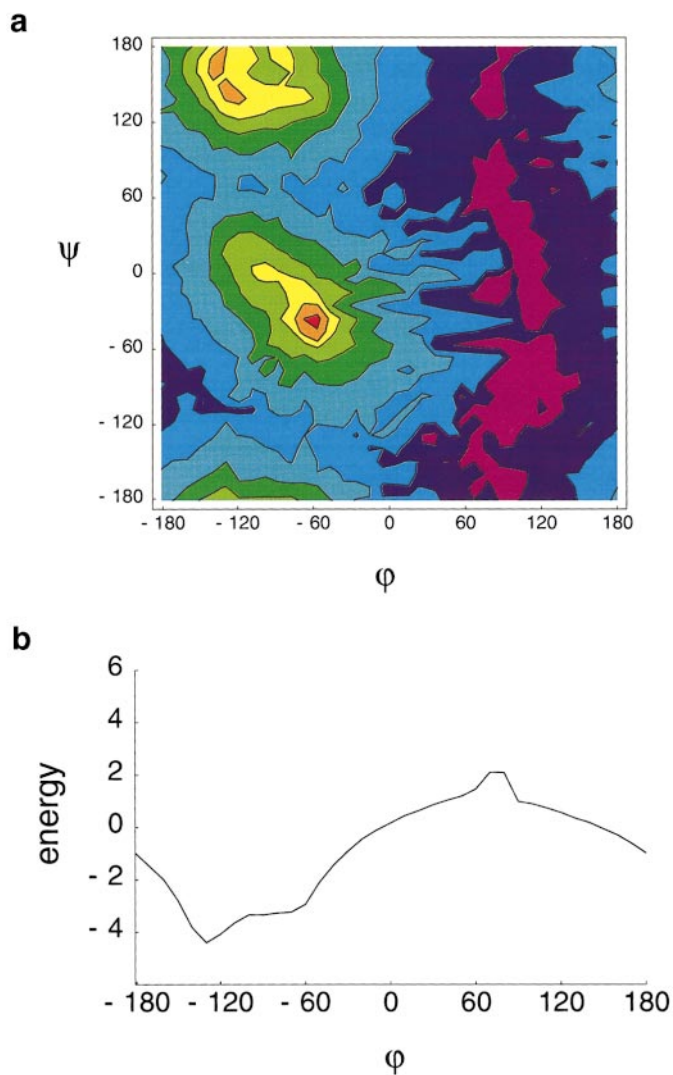


FIG. 1. The DELPHIC torsion potential surface for the backbone ϕ/ψ angles of threonine. (a) The two-dimensional ϕ/ψ potential surface, generated from 638 threonine residues in a database of high-resolution (≤ 1.75 Å) protein crystal structures as described in (3). The surface is color coded from red (low energy) to purple (high energy), with contours drawn in 1 kcal/mol increments. (b) A one-dimensional slice through this potential, taken in the β -sheet region ($\psi = 139^\circ$).

“blockiness” of the potential at this level is an artifact of our implementation. Specifically, the potential of mean force is determined in 10° steps (as described in Ref. 2), and the values at any particular torsion angle value are calculated by linear interpolation from the neighboring grid points. Similarly, the derivative of the potential with respect to the torsion angle is estimated from the local slope of the potential, calculated from the heights of the grid points that surround the particular torsion angle of interest.

Inspection of the Cartesian-space atomic forces that the DELPHIC potential produces yields a surprise: they are extremely rough. Figure 2 shows the magnitude of the force on the backbone nitrogen atom of a threonine residue in the x , y ,

and z directions. The “blockiness” that appeared to be minor in the potential surface is now obvious, and in several places even the direction of the force changes instantaneously. Presumably, these atomic forces are so erratic because the convolution from torsion angle to Cartesian coordinate space magnifies the small inaccuracies of the interpolated potential. Since simulated annealing by means of molecular dynamics assumes that the forces on atoms are continuous, the degree of roughness seen in our original implementation of the DELPHIC torsion potential can obviously cause the type of convergence problem we have noted.

REPLACING THE INTERPOLATED POTENTIAL BY A SUM OF GAUSSIANS

To eliminate the problems associated with the rough derivatives of the interpolated DELPHIC torsion potential, we have replaced the interpolated table of raw potential of mean force values with a sum of fitted Gaussian curves, which are guaranteed to have continuous derivatives. In the two-dimensional case individual Gaussians are of the form

$$\begin{aligned} & \text{gauss}(\text{height}, \text{center}_x, \text{center}_y, \text{width}_x, \text{width}_y, \\ & \quad \text{position}_x, \text{position}_y) \\ & = \text{height} * \exp(-\text{shortestDelta}(\text{center}_x, \\ & \quad \text{position}_x)^2/\text{width}_x) * \exp(-\text{shortestDelta}(\text{center}_y, \\ & \quad \text{position}_y)^2/\text{width}_y) \end{aligned}$$

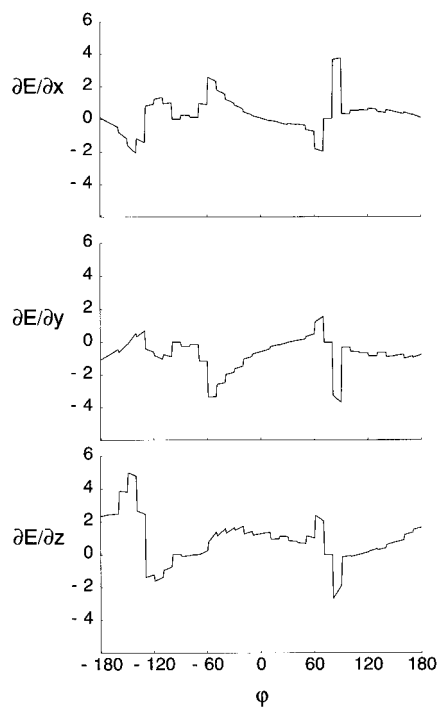


FIG. 2. Forces on the backbone nitrogen atom of threonine generated by the DELPHIC torsion potential as a function of the backbone torsion angle ϕ .

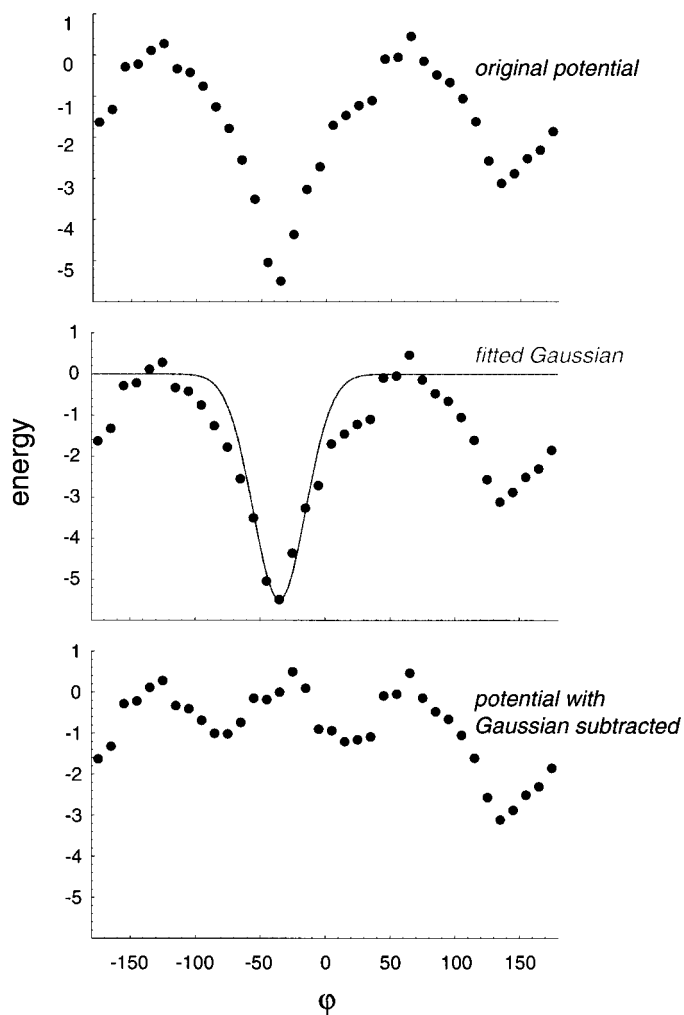


FIG. 3. Illustration of the iterative Gaussian fitting procedure. The top panel shows the original interpolated potential, determined from the potential of mean force in 10° intervals. A Gaussian is fitted to it as described in the text (middle panel) and subtracted off. The remaining potential (lower panel) is then used to fit another Gaussian, and the procedure is repeated. A maximum of 32 Gaussians is used to fit each potential surface.

where height is the height of the Gaussian at its center, its center is defined by center_x and center_y , its width along each axis is defined by width_x and width_y , the position to be evaluated is defined by position_x and position_y , and shortestDelta is given by

$$\text{shortestDelta}(a, b) = \begin{cases} |a - b| & \text{if } |a - b| < 180^\circ, \\ 360^\circ - |a - b| & \text{otherwise.} \end{cases}$$

Similar functions were defined to allow fitting of Gaussians to one-, two-, three-, and four-dimensional potentials of mean force.

Each raw potential of mean force surface is fitted by a sum of these Gaussian functions in the manner illustrated schemat-

ically in Fig. 3. For each Gaussian, the point on the raw potential surface with the greatest absolute value energy is located. Its position gives the center of the new Gaussian, and its energy is its height. Four estimates of the new Gaussian's width are made along each axis, using the energies at the grid points (center-2), (center-1), (center+1), and (center+2), using the equation

$$\begin{aligned} \text{estWidth}(\text{centerPosition}, \text{centerHeight}, \\ \text{neighborPosition}, \text{neighborHeight}) \\ = -\text{shortestDelta}(\text{centerPosition}, \text{neighborPosition})^2 \\ \div \ln(\text{neighborHeight}/\text{centerHeight}) \end{aligned}$$

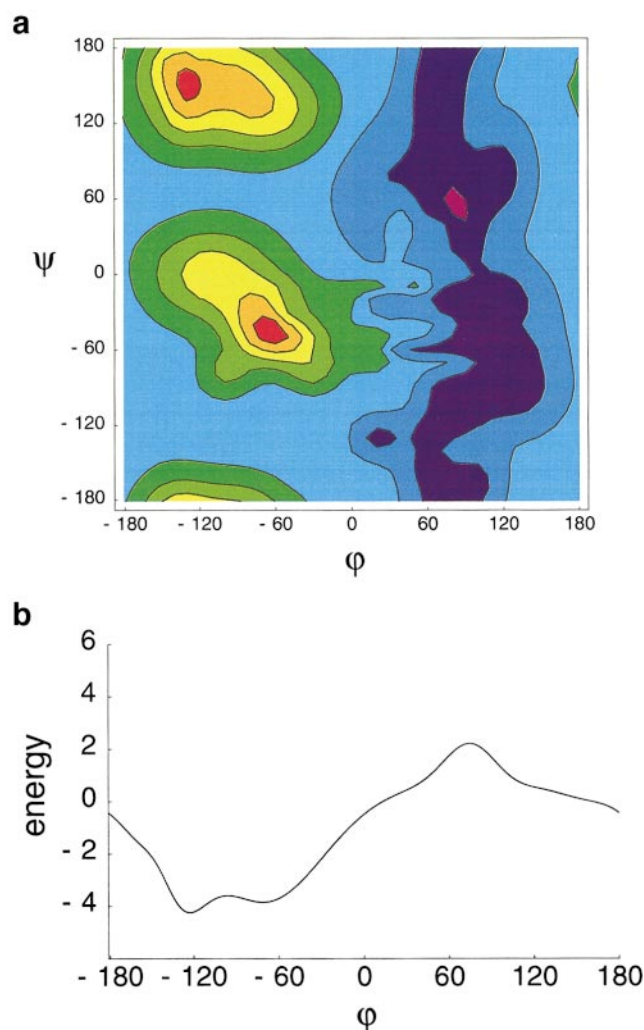


FIG. 4. Example of the Gaussian DELPHIC torsion potential surface. (a) The two-dimensional ϕ/Ψ potential surface for threonine, calculated from the sum of 32 two-dimensional Gaussians fitted as described in the text. (b) A one-dimensional slice through this potential at $\Psi = 139^\circ$, showing, by comparison with Fig. 1b, the detailed agreement of the original interpolated and Gaussian potentials.

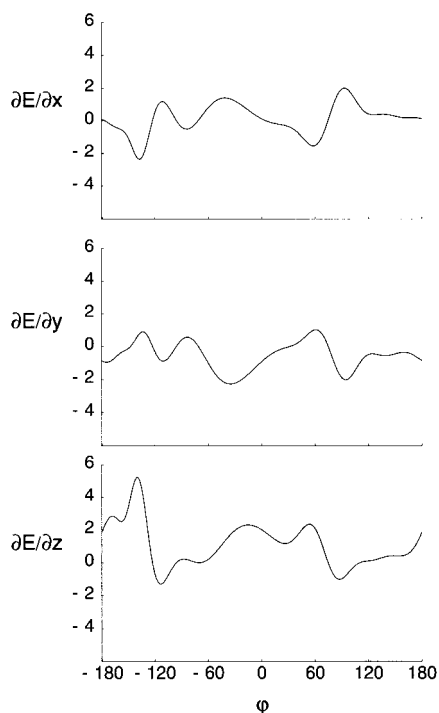


FIG. 5. Forces on the backbone nitrogen atom of threonine generated by the Gaussian DELPHIC torsion potential, as a function of the backbone torsion angle ϕ . Note their similarity to the original forces (Fig. 2), and their reduced extrema in the neighborhood of $\phi = 90^\circ$.

where centerPosition and neighborPosition are the positions of the center of the Gaussian and the neighboring grid point being used to estimate the width, and centerHeight and neighborHeight are the values of the potential of mean force at the center and neighboring grid points. The individual width estimates from the four neighboring grid points along each axis are averaged to give the width of the new Gaussian along that axis. Finally, the value of the new Gaussian at every grid point in the raw surface is subtracted from the raw surface, leaving a new raw potential of mean force. This process was iterated 32 times for each different type of potential surface, yielding 32 Gaussians whose sum reproduces the original interpolated potential with reasonable accuracy.

Inspection of the resulting Gaussian DELPHIC torsion potential surfaces (Fig. 4) shows that the Gaussians reproduce the original potential surface reasonably well, both in overall terms (Fig. 4a) and in detail (Fig. 4b). The Cartesian-space forces on the atoms that the Gaussian DELPHIC torsion potential produces are shown in Fig. 5. Besides being obviously smoother, their magnitudes are very close to those produced by the interpolated potential (Fig. 2), with one exception. In the interpolated potential, the region around $\phi = 90^\circ$ shows a very large discontinuity in the forces, which instantaneously change from large negative to large positive values. The Gaussian DELPHIC potential, in smoothing out this transition, reduces the extreme values of the forces significantly.

TESTING THE GAUSSIAN DELPHIC TORSION POTENTIAL

To evaluate the performance of the Gaussian DELPHIC torsion potential, we calculated a series of structures with the sequence of the B1 domain of streptococcal protein G (5) using a standard Cartesian-space simulated annealing protocol (6) with the program XPLOR (7), comprising 1000 steps (5 fs per step) at 2000 K, followed by 3000 steps (5 fs per step) of cooling down to 100 K, and finally 250 steps of conjugate gradient minimization. No experimental restraints were used in the calculations and the target function comprised terms for the covalent geometry and a quartic van der Waals repulsion term. In addition, a radius of gyration restraint (8) was included to ensure that the coordinates moved significantly from their starting conformation (an extended strand), had realistic packing density, and yielded final structures that included several turn conformations. Twenty structures were calculated with the Gaussian DELPHIC torsion potential, 20 with the interpolated DELPHIC torsion potential, and 20 without the DELPHIC torsion potential.

All the calculated structures had excellent agreement with standard covalent geometry and no van der Waals overlaps. PROCHECK's (7) evaluation of the structures, however, varied widely (Table 1). Structures calculated with no DELPHIC torsion potential only had $21 \pm 6\%$ of their residues in the most favorable regions of the Ramachandran plot, compared to 85 ± 3 and $95 \pm 3\%$ for those calculated with the interpolated and Gaussian DELPHIC potentials, respectively. Although the in-

TABLE 1
Ramachandran Statistics for the Ensemble of Structures Calculated with and without the DELPHIC Torsion Potential^a

Percentage of residues in	No DELPHIC potential	Interpolated DELPHIC potential	Gaussian DELPHIC potential
Most favored regions	21.2 ± 6	85.5 ± 3	94.5 ± 3
Additionally allowed regions	46.6 ± 7	8.4 ± 3	3.6 ± 2
Generously allowed regions	22.9 ± 5	3.5 ± 2	1.6 ± 1
Disallowed regions	9.3 ± 5	2.6 ± 2	0.2 ± 0.6

^a Twenty structures were calculated for each ensemble by simulated annealing, as described in the text and starting from an extended strand ($\phi = -135^\circ$, $\psi = 139^\circ$). The target function in all cases comprises terms for covalent geometry (bonds, angles, and improper torsions), a quartic van der Waals repulsion term to prevent atomic overlap, and a radius of gyration term with a target value of 9.5 \AA . One ensemble was calculated with no DELPHIC torsion angle potential. The other two ensembles were calculated with the DELPHIC torsion angle potential included in the target function for simulated annealing, either in its original interpolated form or in the Gaussian form. The final values of the various force constants are as follows: $1000 \text{ kcal} \cdot \text{mol}^{-1} \cdot \text{\AA}^{-2}$ for bonds, $500 \text{ kcal} \cdot \text{mol}^{-1} \cdot \text{rad}^{-2}$ for angles and improper torsions, $4 \text{ kcal} \cdot \text{mol}^{-1} \cdot \text{\AA}^{-4}$ for the van der Waals repulsion term with the hard-sphere radii set to 0.8 times their value in the CHARMM19/20 parameters, and 20 for the DELPHIC torsion angle potential.

terpolated DELPHIC potential clearly results in a big improvement in the quality of the Ramachandran plot, the simulated annealing schedule is unable to converge to structures with the lowest DELPHIC torsion potential energies. This is due to the presence of rough forces that leave certain residues caught in higher energy conformations, as evidenced by 2–3 and 3–4% of residues remaining in disallowed and generously allowed regions, respectively, of the Ramachandran plot. The significant additional improvement offered by the Gaussian DELPHIC torsion potential (see Table 1) indicates that the smoother forces from the Gaussian surface effectively eliminate the convergence problem.

To evaluate the conformational sampling for the three sets of structures, the mean coordinates for each ensemble were used to best fit each individual structure (Fig. 6). The average backbone root mean square deviation (rmsd) of each structure to its mean coordinate positions provides a measure of conformational sampling, with larger rmsd values indicating better sampling. Structures calculated with no DELPHIC torsion potential had backbone rmsd values of $7.1 \pm 0.7 \text{ \AA}$ to their mean. Surprisingly, structures calculated using the interpolated DELPHIC torsion potential only showed a backbone rmsd value of $4.0 \pm 0.9 \text{ \AA}$. Visual inspection of the structures (Fig. 6) confirms the poor sampling with the interpolated DELPHIC torsion potential. This sampling problem had gone undetected in our previous tests of the interpolated DELPHIC torsion (2, 3) because those earlier calculations were only performed using complete sets of experimental restraints where the inclusion of the interpolated DELPHIC potential did not result in an increase in coordinate precision. The source of the sampling and convergence problems are the same: namely, the rough forces prevent the coordinates from moving easily through certain regions of Ramachandran space, thereby inhibiting full sampling. The structures calculated using the Gaussian DELPHIC torsion potential have a backbone rmsd value of $7.9 \pm 1 \text{ \AA}$, indicating that the smoother forces have eliminated the sampling problems as well.

It should be emphasized that for structures calculated with a large number of NMR restraints, there is little to choose from between the interpolated and Gaussian DELPHIC potentials. For example, in the case of the 33-kDa MEF2A-DNA complex that was solved on the basis of 4560 experimental NMR restraints (including numerous torsion angle restraints) (10), essentially no overall difference can be detected between structures calculated with the interpolated and Gaussian DELPHIC potentials, and both the overall precision of the coordinates ($0.5\text{--}0.6 \text{ \AA}$) and the percentage of residues in the most favorable region of the Ramachandran map (which spans a range of 83–92% with a mean value $\sim 87\text{--}88\%$) are very similar. Where one would clearly expect the Gaussian DELPHIC potential to have a clear cut advantage over the interpolated one would be in cases of structures calculated with very few NMR restraints (11).

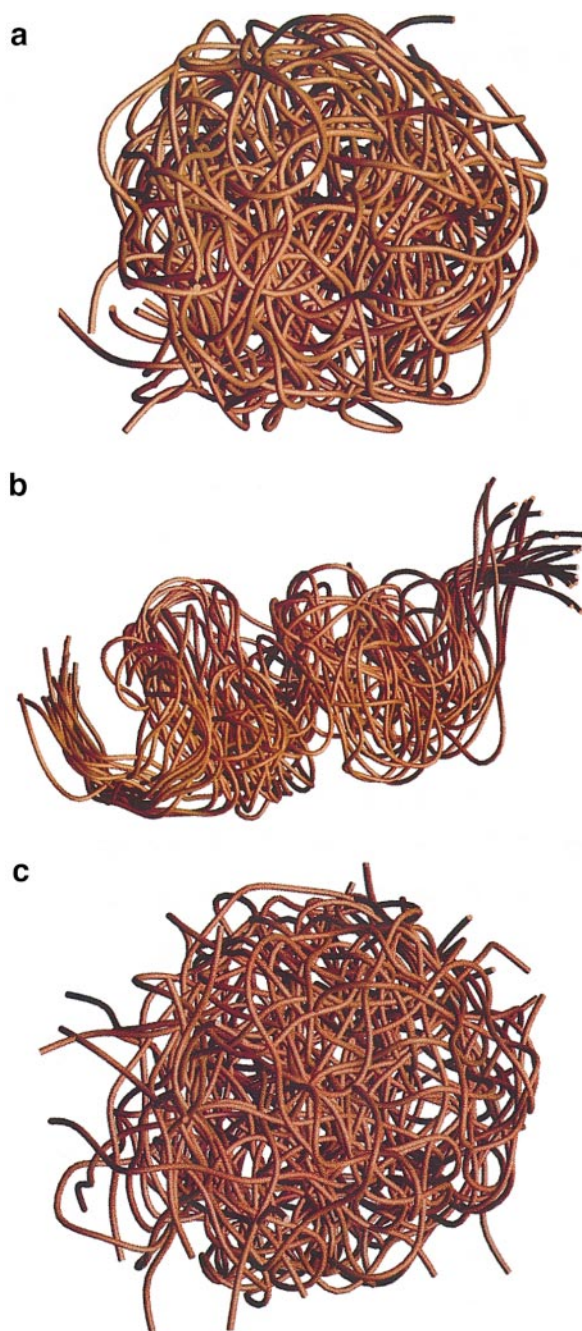


FIG. 6. Ensemble of structures calculated with (a) no DELPHIC torsion potential, (b) the original interpolated DELPHIC torsion potential, and (c) the Gaussian DELPHIC torsion potential. The structures were calculated as described in the text, and are best fitted to the mean coordinate positions of a given ensemble.

CONCLUDING REMARKS

We have uncovered a shortcoming of our original implementation of the DELPHIC torsion potential (2, 3), which seeks to bias structures toward combinations of torsion angles that are commonly seen in protein crystal structures. Our

original implementation produced surprisingly rough forces on the atoms involved in a given torsion angle or groups of torsion angles, which in turn reduced both conformational sampling and convergence to structures with commonly seen torsion angles. This does not present an issue when calculations are carried out with very complete sets of experimental NMR restraints, but does become significant when calculations are carried out with minimal experimental NMR restraints. By replacing our original implementation with one that evaluates the potential energy, and thus the atomic forces it produces, with a sum of several multidimensional Gaussians, we have completely eliminated these rough forces. Smoothing out the atomic forces removes any sampling and convergence problems, resulting in structures that sample all the possibilities that are consistent with the experimental restraints, but which also exhibit torsion angle combinations that are as good as those seen in high-resolution (≤ 1.75 Å) crystal structures. We also expect that the Gaussian DELPHIC potentials will be useful for the refinement of low-resolution X-ray structures of macromolecules.

ACKNOWLEDGMENTS

We thank Frank Delaglio for useful discussions. The complete source code, plus associated files and examples, for the NIH version of XPLOR, which includes the DELPHIC potentials, is available either directly from G.M.C. (clore@speck.niddk.nih.gov) or by anonymous ftp at portal.niddk.nih.gov in the directory /pub/clore/xplor_nih.

REFERENCES

1. G. M. Clore and A. M. Gronenborn, New methods of structure refinement for macromolecular structure determination by NMR, *Proc. Natl. Acad. Sci. U.S.A.* **95**, 5891–5898 (1998).
2. J. Kuszewski, A. M. Gronenborn, and G. M. Clore, Improving the quality of NMR and crystallographic protein structures by means of a conformational database potential derived from structure databases, *Prot. Sci.* **5**, 1067–1080 (1996).
3. J. Kuszewski, A. M. Gronenborn, and G. M. Clore, Improvements and extensions in the conformational database potential for the refinement of NMR and X-ray structures of proteins and nucleic acids, *J. Magn. Reson.* **125**, 171–177 (1997).
4. M. J. Sippl, Calculation of conformation ensembles from potentials of mean force: An approach to the knowledge-based prediction of local structures in globular proteins, *J. Mol. Biol.* **213**, 859–883 (1990).
5. A. M. Gronenborn, D. R. Filpula, N. Z. Essig, A. Achari, M. Whitlow, P. T. Wingfield, and G. M. Clore, A novel, highly stable fold of the immunoglobulin domain of streptococcal protein G, *Science* **253**, 657–661 (1991).
6. M. Nilges, G. M. Clore, and A. M. Gronenborn, Determination of three-dimensional structures of proteins from interproton distance data by hybrid distance geometry-dynamical simulated annealing calculations, *FEBS Lett.* **229**, 317–324 (1988).
7. A. T. Brünger, "XPLOR: A System for NMR and Crystallography," Yale Univ. Press, New Haven, CT (1992).
8. J. Kuszewski, A. M. Gronenborn, and G. M. Clore, Improving the packing and accuracy of NMR structures with a pseudopotential for the radius of gyration, *J. Am. Chem. Soc.* **121**, 2337–2338 (1999).
9. R. A. Laskowski, M. W. MacArthur, D. S. Moss, and J. M. Thornton, PROCHECK: A program to check the stereochemical quality of protein structures, *J. Appl. Cryst.* **26**, 283–291 (1993).
10. K. Huang, J. M. Louis, L. Donaldson, F.-L. Lim, A. D. Sharrocks, and G. M. Clore, Solution structure of the MEF2A-DNA complex: Structural basis for the modulation of DNA bending and specificity by MADS-box transcription factors, *EMBO J.* **19**, 2615–2628 (2000).
11. G. M. Clore, M. R. Starich, C. A. Bewley, M. Cai, and J. Kuszewski, Impact of residual dipolar couplings on the accuracy of NMR structures determined from a minimal number of NOE restraints, *J. Am. Chem. Soc.* **121**, 6513–6514 (1999).